Microchemical Journal 229 (2026) 119269

Contents lists available at ScienceDirect

Microchemical Journal

journal homepage: www.elsevier.com/locate/microc

Analytical determination of cannabinoids in *Cannabis Sativa L.*: the key role of boric acid complexation

Filippo Lugli, Alessandro Monari, Monica Caselli, Erika Ferrari, Davide Vanossi, Iuri Camilli, Martina Campi, Laura Pigani *

Department of Chemical and Geological Sciences, University of Modena and Reggio Emilia, via G. Campi 103, 41125 Modena, Italy

ARTICLE INFO

Keywords:
Cannabinoids
Boric acid complexes
Voltammetry
Fluorescence
^{11}B NMR

ABSTRACT

The electrochemical discrimination of cannabinoids remains a major challenge in electroanalytical sensing due to their structural similarity and overlapping redox behaviour. This study demonstrates that boric acid enables the selective detection of acidic cannabinoids Δ^9-tetrahydrocannabinolic acid (Δ^9-THCA) and cannabidiolic acid (CBDA) through the formation of an intramolecular borate chelate. At neutral pH, boric acid forms a tetrahedral borate complex through anchoring at the carboxylate group and coordination at the phenolic oxygen, stabilizing a six-membered metallacycle. This complexation induces distinct analytical signatures, including the emergence of a high-potential oxidation peak in differential pulse voltammetry, a blue-shifted and enhanced fluorescence emission, and characteristic ^{11}B NMR shifts. Neutral analogues (Δ^9-THC, CBD) do not undergo complexation and therefore lack these features. The integrated voltammetric, fluorometric, and NMR data elucidate the molecular basis of borate-induced selectivity and provide a mechanistic foundation for the rational design of electrochemical sensors for forensic and regulatory applications.

1. Introduction

Over the past decade, the trafficking and consumption of illicit drugs have steadily increased, presenting global challenges due to their impact on society, public health, criminal activities, and the environment.

To address these issues, the development of rapid and reliable on-site drug detection methods is essential. In this context, electrochemical sensors have shown significant potential as an alternative to traditional chromatographic and spectroscopic techniques, as well as to point-of-care immunoassay-based testing and portable colorimetric tests, thanks to their low cost and portability [1]. Furthermore, the functionalization of electrodes with suitable (nano)materials enhances the sensitivity required for trace detection in accordance with regulatory standards, while also improving selectivity to minimise interferences.

Focusing on *Cannabis sativa* L., it is one of the most widely used drugs in Europe, with 23% of young adults and adults reporting use within the past year [2]. Its psychotropic effects stem from Δ^9-tetrahydrocannabinol (Δ^9-THC), which can induce euphoria, anxiety, somnolence, altered visual and auditory perception, and impaired psychomotor performance [3]. Due to these effects, its use is legally regulated in most countries worldwide. Conversely, the favourable pharmacological properties of cannabidiol (CBD) have driven its widespread use in therapeutic and commercial products [4].

A wide variety of cannabis strains are now available, exhibiting different potencies, which depend on the concentration of Δ^9-THC and its ratio to CBD within each strain. Some strains can contain Δ^9-THC levels as high as to 18% *w*/w, reflecting a steady increase since the 1990s, when the average Δ^9-THC content of seized *C. sativa* was around 6–8% *w*/w [5,6]. In addition to higher concentrations of Δ^9-THC, these newer high-potency *C. sativa* strains typically exhibit reduced or negligible CBD concentrations [6–8]. On the other hand, the cultivation of fiber-type *C. sativa*, with high CBD levels and negligible Δ^9-THC content, is now permitted across the European Union, and hemp-derived oils and derived medical products are widely available in pharmacies [9,10]. This evolving landscape highlights the need for effective sensor systems capable of accurately measuring Δ^9-THC and CBD levels in both biological samples and plant material.

It is worth noting that cannabinoids are biosynthesized in their acidic forms within plant tissues; thus, Δ^9-tetrahydrocannabinol acid (Δ^9-THCA) and cannabidiol acid (CBDA) are the only forms produced directly by the *C. sativa* plant [11,12] and are therefore the predominant forms found in plant samples. Δ^9-THCA and CBDA can undergo

* Corresponding author.
E-mail address: laura.pigani@unimore.it (L. Pigani).

https://doi.org/10.1016/j.microc.2026.119269
Received 16 April 2026; Received in revised form 27 July 2026; Accepted 2 August 2026
Available online 3 August 2026

spontaneous decarboxylation, yielding their neutral counterparts upon exposure to heat, light, and oxygen [13,14].

To date, several amperometric sensors [15–19] have been developed for the detection of cannabinoids, particularly Δ^9-THC, given its psychotropic activity. The electrochemical detection of cannabinoids exploits the presence of an oxidizable phenolic group, whose oxidation is favoured at carbon-based electrodes. Selectivity is commonly enhanced by using voltammetric techniques such as differential pulse voltammetry and square wave voltammetry, which improve the signal-to-noise ratio. According to the mechanism reported in the literature [16,17], Δ^9-THC, similarly to other phenolic compounds, undergoes oxidation forming an unstable phenoxy radical, which rapidly reacts, generating undefined by-products that can lead to electrode passivation. Additional oxidation pathways, such as those involving the ether moiety, may also occur. An alternative mechanism leading to the formation of a quinone has been proposed [18,19].

Recently, the attention of our research group has been focused on the development of amperometric systems for the rapid discrimination between legal and illegal *C. sativa* samples [20,21]. Since this distinction relies primarily on the content of the psychoactive cannabinoid, the analytical challenge lies in generating sufficiently different electrochemical responses for Δ^9-THC/Δ^9-THCA and CBD/CBDA. However, the structural similarity of main cannabinoids often results in nearly overlapping voltammetric signals, limiting selectivity.

To address this challenge, the use of boric acid (H_3BO_3) as a means to modulate the electrochemical behaviour of acidic cannabinoids was explored. It is well established that H_3BO_3 can form complexes with aliphatic molecules bearing *cis*-vicinal diols, with catechol and its derivatives, and with α-hydroxy acids [22–26]. Usually, dioxygenated chelators such as salicylic acid react directly with the trigonal boric acid thanks to the carboxylic anchoring group that favours the following substitution of a hydroxy group in coordination sphere of boron with the a-hydroxy oxygen of the chelator. The boron complex is characterized by a tetrahedral geometry [27,28]. In the case of catechol and caffeic acid, it has been shown that, in the presence of boric acid, two distinct oxidation peaks appear in the voltammograms, presumably corresponding to the free analyte and its borate-complex [29–31].

This work investigates how boric acid, introduced through a Britton–Robinson buffer, modulates the electrochemical behaviour of the acidic cannabinoids Δ^9-THCA and CBDA. The goal is to determine whether borate complexation can generate distinguishable electrochemical signatures that enable selective detection of these analytes. To this end, a comprehensive electrochemical study of Δ^9-THCA and CBDA in presence of boric acid/borate was conducted, including the set-up of the experimental conditions and the comparison with the decarboxylated counterparts, i.e. Δ^9-THC and CBD. To elucidate the interaction mechanism between acidic cannabinoids and boric acid, voltammetric measurements were complemented by fluorescence spectroscopy and ^{11}B NMR. Furthermore, model compound (2,5-dihydroxybenzoic acid) was used as benchmark to confirm the B-complex structure and the role of the chelating moiety. Although several studies have been reported on the fluorescence properties of cannabinoids, particularly intense for the acidic forms [32–34], to date no investigations have been carried out in the presence of H_3BO_3. Fluorescence spectroscopy thus offers an excellent opportunity to gain further insight into the interaction between acidic cannabinoids and boric acid. At the same time, ^{11}B NMR spectroscopy represents a powerful technique able to easily discriminate between boron complexes with different molar ratios, as the ^{11}B chemical shift is sensitive to changes in the coordination sphere with a downfield shift of the signal (higher chemical shift) when the metal-to-ligand ratio rises [35].

The insights gained from this study will support the development of reliable sensor technologies capable of distinguishing between psychoactive and non-psychoactive cannabis constituents, thereby contributing to public health, regulatory compliance, and forensic applications.

2. Experimental

2.1. Instrumentation

All electrochemical measurements were performed with an Autolab PGSTAT128N (Eco Chemie, Utrecht, The Netherlands), under the control of NOVA 2.1 software. Voltammetric measurements were performed using commercial Screen-Printed Electrodes (SPEs) acquired from Sense4Med (Rome, Italy). These SPEs consist of a 0.07 cm^2 graphite working electrode, a graphite auxiliary electrode, and an Ag pseudo-reference electrode. Carbon black (CB) N220 was used for the modification of the SPEs; the CB was deposited on the working electrode surface by drop-casting, from a 1 mg/mL suspension obtained in a 1:1 (v/v) DMF (Scharlau, 99.8%) and deionized water. Three consecutive drops of 2 μL each were deposited on the SPEs. The electrodes were allowed to dry in air at room temperature after the drop-casting of each drop.

UV–vis spectra were collected using an Agilent Varian Cary 100 Scan UV–vis spectrophotometer.

Fluorescence spectra were measured with a Horiba FluoroMax-4 spectrofluorometer.

^{11}B NMR spectra were recorded on an Avance AMX 600 spectrometer equipped with a CryoProbe BBO H&F 5 mm in inverse detection mode (nominal frequency of 192.55 MHz). Chemical shifts (δ) are reported in parts per million (ppm). In order to remove ^{11}B background due to boron-silicate glass of regular 5 mm NMR tubes, 4 mm quartz tubes were used for the acquisition, instead.

2.2. Reagents and solutions

All the solutions were prepared using deionized water (18 MΩ•cm resistivity). A 0.1 M phosphate buffer (PB) was prepared by dissolving 8.54 g of sodium dihydrogen phosphate monohydrate ($NaH_2PO_4{\cdot}H_2O$, Calbiochem, 98%) and 5.41 g of anhydrous disodium hydrogen phosphate (Na_2HPO_4, Carlo Erba, 98%) in deionized water and diluting to a final volume of 1 L. If necessary, the pH was adjusted to 7.0 by addition of a few drops of 3 M sodium hydroxide (NaOH, Fisher Chemical, 98.3%) or 3 M hydrochloridic acid (HCl, Carlo Erba, 37%).

A 0.12 M Britton–Robinson buffer (BRB) was prepared from 0.04 M boric acid (H_3BO_3, Carlo Erba, 99.8%), 0.04 M sodium acetate (CH_3COONa, Carlo Erba, 99.5%), and 0.04 M NaH_2PO_4. The pH was adjusted to the desired value by dropwise addition of 3 M NaOH or 3 M HCl.

Potassium chloride (KCl, Sigma Aldrich, ≥99.0%) was added to each buffer solution to obtain a final concentration of 0.1 M. Deuterium oxide (D_2O) and acetonitrile (ACN; Carlo Erba) have been used for the ^{11}B NMR tests. Standard solutions of CBDA, CBD, Δ^9-THCA, and Δ^9-THC (1 mg/mL, either in acetonitrile or methanol) were purchased from Cerilliant, and 2,5-dihydroxybenzoic acid (99%) was purchased from Thermo Fisher Scientific.

Two samples of *C. sativa* female inflorescences, available at the Toxicology Laboratory of the Forensic Institute of the Department of Biomedical, Metabolic and Neural Sciences of the University of Modena and Reggio Emilia, were analysed. The samples were classified as R1 (recreational/illegal) and F1 (fiber/legal), on the base of HPLC analysis of their ethanolic extracts. Specifically, sample R1 contained 30.96 mg/g of Δ^9-THC and 172.31 mg/g of Δ^9-THCA, corresponding to a total Δ^9-THC content of 18.02%. Sample F1 contained 17.6 mg/g of CBD, 46.83 mg/g of CBDA, and 1.83 mg/g of Δ^9-THC, corresponding to a total Δ^9-THC content of 0.18%.

2.3. Electroanalytical tests

Cyclic Voltammetry (CV) and Differential Pulse Voltammetry (DPV) were used to perform electrochemical analyses of CBDA, CBD, Δ^9-THCA, and Δ^9-THC as well as 2,5-dihydroxybenzoic acid (2,5-DHBA). All the electroanalytical tests were carried out in a 7:3 *v*/v mixture of buffer

solution (BRB or PB) and ethanol (EtOH, ≥ 99.8% Sigma Aldrich), containing 0.1 M KCl, freshly prepared on a daily basis. Ethanol was introduced as a co-solvent to enhance the solubility of cannabinoids, which are poorly soluble in purely aqueous media, while maintaining sufficient buffer capacity to control the pH during measurements. The selected 7:3 buffer–ethanol ratio represents a compromise between analyte solubility and the maintenance of suitable electrochemical conditions [36,37]. KCl was added to all solutions employed to promoting the formation in situ of a Ag/AgCl pseudo-reference electrode; all the potentials reported hereafter will be referred to this redox couple.

When preparing diluted solutions from cannabinoids standards, a suitable volume of EtOH was added to the required volume of the standard to reach a final volume of 30 μL; then, 70 μL of buffer solution were added. To prepare diluted solutions of 2,5-DHBA, a very similar procedure was used, starting this from a mother solution in deionized water of the selected analyte. The *C. sativa* extracts were diluted 10 times; 10 μL of extracts were mixed to 20 μL of EtOH and 70 μL of buffer to keep the 7:3 H_2O-EtOH volume proportion. The use of the same electrolyte composition for both standard solutions and plant extracts ensures consistency, thereby enhancing the reliability and comparability of the results.

DPV was used with the following parameters: 50 mV pulse potential, 6 mV step potential, 0.1 s pulse time, and 0.4 s interval time (corresponding to a 15 mV/s potential scan rate). Before each measurement, all the SPEs-CB underwent 10 DPV scans in a blank solution formed by a 7:3 v/v mixture of buffer and EtOH containing 0.1 M KCl, to stabilize the background signal. After that, the voltammograms recorded consisted of five consecutive DPV scans in the potential range between 0.0 and +1.1 V. Each solution was analysed with a new SPE-CB.

2.4. UV–vis absorption and fluorescence tests

UV–vis spectra were recorded with quartz cuvettes (1 cm path length). pH-dependent UV–vis spectrophotometric titrations were carried out using the in-cell method, data were collected at $T = 25$ °C and 0.10 M NaCl. pH measurements were performed using a calibrated pH meter (Mettler-Toledo). The ligand solution ($C_L = 30$ mM and 100 mM for Δ^9-THCA and 2,5-DHBA, respectively) was added of negligible volumes (μL) of HCl and/or NaOH to adjust the pH. The electronic spectra were recorded, and the equilibrium was considered to be reached when no further changes in either the pH or the electronic spectra were observed. The thermodynamic data were elaborated with HypSpec, HySS and PyES [38–40].

Fluorescence spectra were measured using 0.4 × 1.0 cm quartz cuvettes (1 cm path length) and acquired with right-angle detection. The excitation and emission slit widths were set at 2 and 3 nm, respectively. The value of the absorbance of the samples at the excitation wavelength was less than 0.2. The fluorescence spectra of Δ^9-THCA and CBDA were corrected for the instrumental spectral sensitivity, after the subtraction of the buffer signal. Measurements were performed in 7:3 v/v mixture of 0.024 M BRB or 0.01 M PB (each one at pH = 7.0) and EtOH. The absorption and fluorescence spectra recorded in BRB at increasing boric acid concentrations were obtained in 0.012 M BRB and 0.004 M H_3BO_3. The use of diluted buffer solutions, compared with those employed in the electrochemical tests, was necessary to prevent the formation of suspensions.

2.5. ^{11}B NMR analysis

The ^{11}B NMR spectrum of boric acid/borate (blank) was obtained by adding 450 μL of 10 mM H_3BO_3 solution prepared in PBS (0.1 M, pH = 7) and 50 μL of D_2O into a 4 mm quartz tube.

The system B(III)-2,5-DHBA was investigated in PBS solution (0.1 M, pH = 7) in the 1-to-1 and 1-to-2 metal-to-ligand molar ratios ($C_B = 10$ mM; $C_L = 10$ mM and 20 mM). 450 mL of the PB B(III)-2,5-DHBA solution were spiked with 50 mL of D_2O for deuterium locking purposes. Due to the low solubility of cannabinoids in water, Δ^9-THCA sample was prepared in 7:3 *v*/v mixture of PB buffer (0.1 M, pH = 7.0) and ACN. 450 mL of the mixture containing H_3BO_3 and Δ^9-THCA ($C_B = 20$ mM; $C_L = 1.3$ mM) were spiked with 50 mL D_2O and analysed.

3. Results and discussion

3.1. Boron complexation

To elucidate the molecular basis of the interaction between acidic cannabinoids and boric acid, a preliminary spectroscopic investigation was undertaken to characterize their acid–base behaviour and evaluate their ability to form borate complexes.

Δ^9-THCA is a weak biprotic acid, namely H_2L, characterized by the first proton dissociation of the carboxylic group ($pK_{a,1}$) followed by the dissociation of phenolic one ($pK_{a,2}$). Since to our best knowledge the protonation equilibria of Δ^9-THCA have never been reported in the literature, the proton dissociation constants of Δ^9-THCA and, for comparison, 2,5-DHBA have been calculated through UV–vis spectroscopy data (Fig. SI1). The results are summarized in Table 1, together with those of salicylic acid (SA).

Around neutral pH the prevailing species in solution for Δ^9-THCA is HL^- in which the carboxylic group is fully dissociated while the phenolic group is undissociated (Fig. SI2). A similar behaviour is observed for 2,5-DHBA. The dissociation constants, particularly the carboxylic one, suggest a decreased acidity of Δ^9-THCA in comparison to 2,5-DHBA, probably due to the presence of the alkyl substituent in *ortho* position in the aromatic ring instead of the hydroxyl one [41].

Since the pK_a of H_3BO_3 is 9.05 [27], at neutral pH, the prevailing species of boron will be the form $B(OH)_3$. When Δ^9-THCA is present together with $B(OH)_3$ at pH ≈ 7, the deprotonated carboxyl group may interact with boron through a negatively charged carboxylate oxygen, providing an anchoring point that preorganizes the ligand and brings the neighbouring phenolic OH group into proximity with the boron center. Since neutral phenolic hydroxyl groups are weak donors toward boron (III), coordination is expected to become significant only upon phenolic deprotonation. The stabilization of the resulting boron–phenolate interaction, combined with chelate formation and intramolecular preorganization, can rationalize the observed increase in phenolic acidity, expressed as a decrease in the phenolic pK_a. This process ultimately leads to a six-membered boron-containing chelate ring involving coordination of both the carboxylate and phenolate oxygen atoms (Fig. 1).

In large excess of $B(OH)_3$ at neutral pH, the prevailing boron-complex is supposed to be the 1-to-1 metal-to-ligand $[BL]^-$. A similar behaviour can be predicted for 2,5-DHBA.

The proposed mechanism provides a base for interpreting the electrochemical and photophysical effects examined in the following sections.

3.2. Electrochemical study

To investigate whether borate–cannabinoid complexation can modulate the voltammetric response, it is essential to perform

Table 1
Acidity constants (pK_a) of Δ^9-THCA and 2,5-DHBA ($T = 25$ °C, $I = 0.10$ M NaCl). Literature data for salicylic acid (SA) are reported for comparison purposes. pK_a values are calculated from experimentally refined $\log\beta_{LH}$ values.

	Δ^9-THCA*	2,5-DHBA**	SA[a]
$pK_{a,3}$	/	12.0 ± 0.01	/
$pK_{a,2}$	10.96 ± 0.01	9.84 ± 0.02	13.61
$pK_{a,1}$	5.09 ± 0.02	2.61 ± 0.05	2.98

* $pK_{a,1} = \log\beta_{12} - \log\beta_{11}$; $pK_{a,2} = \log\beta_{11}$.
** $pK_{a,1} = \log\beta_{13} - \log\beta_{12}$; $pK_{a,2} = \log\beta_{12} - \log\beta_{11}$; $pKa_{,3} = \log\beta_{11}$.
[a] Taken from Ref. [35].

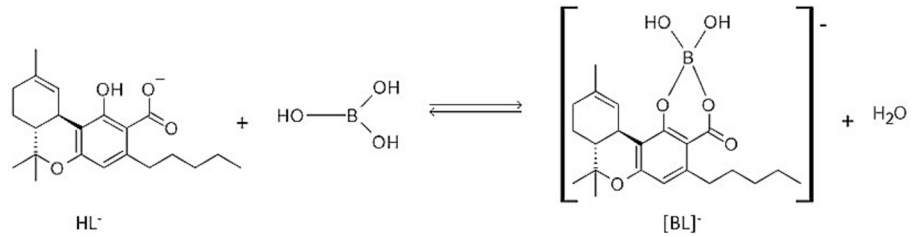

Fig. 1. Formation reaction of the boron-(Δ^9-THCA) complex.

electrochemical measurements both in the presence and in the absence of boric acid. Because cannabinoids exhibit very limited solubility in water, all experiments were carried out in in a 7:3 (v/v) hydroalcoholic medium, previously identified as optimal for electrochemical investigations of these compounds [37]. This solvent composition is particularly advantageous here, as it allows boric acid to be introduced directly as a component of the buffer—analogously to what occurs in BRB—while still enabling straightforward substitution of the buffer when measurements without borate are required for comparison. Regardless of the buffer formulation, maintaining a neutral pH ensures optimal analytical performance for all cannabinoids in terms of peaks intensity, consistent with earlier findings for cannabinol and CBD [36,37] and further confirmed for Δ^9-THCA and CBDA (Fig. SI3). Fig. 2 shows the DPV responses of Δ^9-THC, Δ^9-THCA, CBD and CBDA, recorded respectively using BRB (red lines) or PB (black lines) at pH = 7.0.

Comparing the plots shown in Fig. 2, it is clearly evident that despite the structural similarity of the cannabinoids, their electrochemical signals are significantly different, especially when measurements are performed using BRB. For Δ^9-THC (Fig. 2A) the voltammetric response is essentially identical in BRB and PB, displaying a single oxidation peak at +0.38 V. This process is consistent with the oxidation of the phenolic moiety to the corresponding *p*-quinone, as reported in the literature [19]. The absence of any change upon addition of borate indicates that Δ^9-THC does not significantly interact with borate under these conditions.

In contrast, Δ^9-THCA (Fig. 2B) exhibits a more complex behaviour. In both buffers, a first oxidation peak appears at approximately +0.50 V, shifted by about +100 mV relative to Δ^9-THC. This anodic shift can be attributed to the electron-withdrawing effect of the carboxylic group, which stabilizes the molecule and makes oxidation thermodynamically less favourable. Notably, in BRB only, a second high-potential oxidation peak emerges at +0.82 V. The appearance of this additional signal

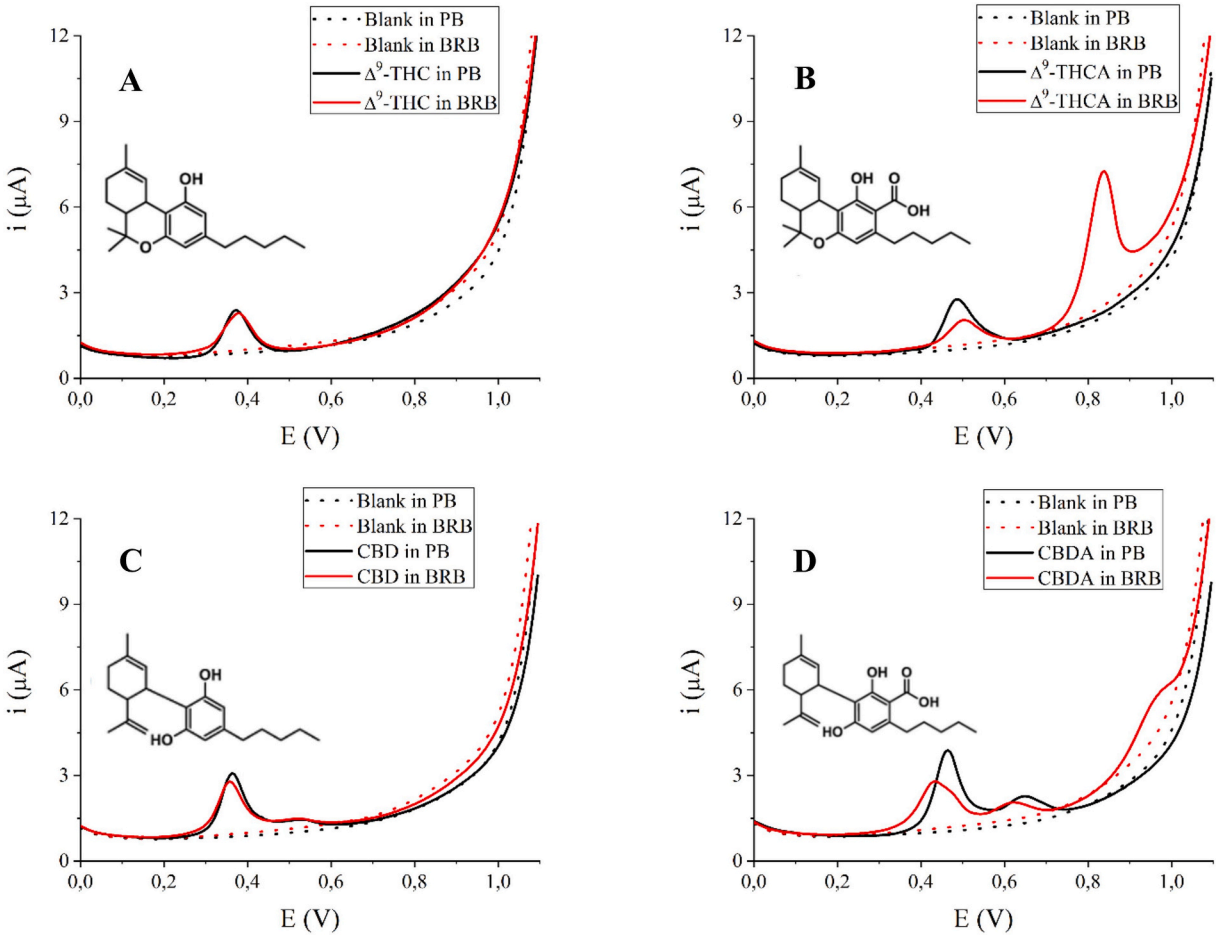

Fig. 2. DPV signals recorded using SPE-CB in a 7:3 v/v mixture of BRB or PB (pH = 7.0) and EtOH, 0.1 M KCl in the presence of A) 50 μM Δ^9-THC; B) 50 μM Δ^9-THCA; C) 50 μM CBD; D) 50 μM CBDA.

strongly suggests the formation of borate–Δ^9-THCA complexes. Such complexation alters the electronic environment of the molecule, enabling an additional oxidation pathway at higher potential.

A similar trend is observed for CBD and CBDA (Fig. 2C and D). CBD exhibits two near oxidation peaks in both buffers, the main one located at +0.37 V, consistent with literature reports that attribute these signals to distinct oxidation pathways involving the two phenolic groups and subsequent chemical transformations [19]. The fact that these peaks are nearly unaffected by the buffer composition indicates that CBD does not significantly interact with borate. Conversely, CBDA shows clear buffer-dependent differences. Its first main oxidation peak appears at approximately +0.44 V, again shifted anodically relative to CBD due to the electron-withdrawing effect of the carboxyl group. Importantly, a new high-potential oxidation peak at approximately +0.95 V is observed exclusively in BRB. As in the case of Δ^9-THCA, this behaviour supports the formation of borate–CBDA complexes, which give rise to an additional oxidation process at higher potential.

The comparison between PB and BRB further reveals differences in peak intensities. For both Δ^9-THCA and CBDA, the first oxidation peak is generally more intense in PB, whereas the peak at higher potential appears only in BRB. This suggests that, in the presence of borate, an equilibrium is established between free and complexed species.

Table 2 summarizes the peak potential values measured in PB and BRB for all four cannabinoids.

Overall, these results demonstrate that borate plays a selective role in modulating the electrochemical response of acidic cannabinoids (Δ^9-THCA and CBDA), while neutral cannabinoids (Δ^9-THC and CBD) remain largely unaffected. This behaviour is consistent with the ability of borate to form stable complexes with suitably arranged oxygen-containing functional groups, providing strong evidence that borate–cannabinoid interactions are responsible for the additional oxidation processes observed in BRB.

To further probe the hypothesis that boric acid is directly involved in generating the high-potential peak of Δ^9-THCA or CBDA, additional experiments were performed by adding boric acid to a 7:3 v/v mixture of PB (pH 7.0) and EtOH containing Δ^9-THCA. As shown in Fig. SI4, the peak at +0.82 V emerges upon addition of H_3BO_3 and increases with its concentration, unequivocally confirming the key role of boric acid in producing this second voltammetric signal. A complementary study was carried out using 2,5-DHBA as a simpler model compound containing the same functional groups potentially involved in complexation with H_3BO_3. As previously observed for Δ^9-THCA, the addition of H_3BO_3 caused a progressive enhancement of a second oxidation peak, as shown in Fig. SI5. This behaviour indicates a concentration-dependent interaction, likely shifting the equilibrium toward a borate complex oxidizing at higher potentials [42].

It is interesting to note that the differences in the voltametric signals in BRB were found to be highly significant for the identification of Δ^9-THCA and CBDA in cannabis sample extracts, and they formed the basis of the classification models used to discriminate between legal and illegal cannabis samples, developed in our previous work [21]. In particular, the presence of the second intense Δ^9-THCA peak at +0.82 V enabled the identification of this analyte, the precursor of psychotropic Δ^9-THC, directly in plant samples. The analytical relevance of the second anodic peak is illustrated in Fig. 3, which compares DPV profiles of two cannabis extracts: R1, rich in Δ^9-THCA (recreational/illegal), and F1, rich in CBDA with low Δ^9-THCA (fiber/legal). It is well established that both the profile and concentration of cannabinoids in cannabis plants can vary substantially. Nevertheless, based on the analysis of a large number of extracts, a consistent pattern emerged. Specifically, recreational cannabis samples are generally characterized by very high concentrations of Δ^9-THC and Δ^9-THCA, accompanied by low levels of CBD and CBDA. In contrast, fiber-type cannabis samples exhibit very low concentrations of Δ^9-THC and Δ^9-THCA, together with high, often very high, concentrations of CBD and CBDA. On this basis, samples R1 and F1 can reasonably be considered representative of illicit and legal cannabis classes, respectively.

Table 2
Peak potentials obtained by DPV technique in BRB and PB for the four cannabinoids.

Molecule	BRB		PB	
	1st peak	High-potential peak	1st peak	High-potential peak
Δ^9-THC	+0.38 V	/	+0.38 V	/
Δ^9-THCA	+0.50 V	+0.82 V	+0.48 V	/
CBD	+0.37 V	/	+0.37 V	/
CBDA	+0.44 V	+0.95 V	+0.47 V	/

When BRB is used, the overall voltammetric profiles of R1 and F1 samples closely resemble those of the main cannabinoids present in each one of them (Fig. 3A), supporting the validity of the electrochemical fingerprint. The R1 extract exhibits a first signal characterized by shoulder at ca. +0.40 V, compatible with the oxidation potential of Δ^9-THC, followed by a peak at +0.50 V, corresponding with the first oxidation potential of Δ^9-THCA. A second characteristic high-potential peak at approximately +0.84 V unequivocally attributable to Δ^9-THCA, thus enabling rapid identification of illegal samples. The F1 sample presents a system of peaks between +0.30 and +0.70 V, consistent with the oxidation of CBD and CBD, along with a small peak at approximately +0.96 V attributable to CBDA.

By contrast, in PB the voltammetric profiles of R1 and F1 nearly overlap and are therefore not distinguishable (Fig. 3B). These observations confirm the electrochemical impact of borate complexation and underscore its practical value for cannabis screening.

3.3. UV–vis absorption and fluorescence study

Emission spectroscopy represents an excellent tool to gain additional information on the interaction between acidic cannabinoids and boric acid. For this purpose, electronic absorption and emission measurements were performed on all four cannabinoids (Δ^9-THCA, CBDA, Δ^9-THC, and CBD) under experimental conditions identical to those used for the electrochemical analyses, using the two different buffers, BRB and PB, at pH = 7.0. It should be noted that the buffer concentrations used in the fluorescence experiments were lower than those adopted in the electrochemical tests, in order to prevent particulate formation, which could interfere with the recorded spectra. Remarkably, even under these experimental conditions, voltammograms very similar to those reported in Section 3.2 were obtained.

The UV–vis absorption spectra recorded in the 7:3 v/v mixture of BRB or PB at pH = 7.0 and EtOH for Δ^9-THCA, CBDA, Δ^9-THC, and CBD are reported in Fig. SI6. Changing the buffer nature does not result in significant differences in the shape of the absorption spectra for all cannabinoids. Δ^9-THCA and CBDA exhibit very similar absorption spectra, with maxima at 222, 259, and 300 nm and 223, 257, and 300 nm, respectively. The lowest energy absorption bands in the spectra of Δ^9-THC and CBD are blue-shifted with respect to those of Δ^9-THCA and CBDA. These bands are structured and centred at about 275–280 nm. These results agree with those reported in the literature [32–34] and indicate that Δ^9-THCA and CBDA, on the one hand, and Δ^9-THC and CBD, on the other, show absorption properties similar within each pair. The nature of the electronic transitions responsible for the absorption bands of the four compounds under investigation will be addressed in a future study.

The same solutions used for the UV–vis analyses were used to obtain the fluorescence spectra, which are shown in Fig. 4. The fluorescence spectra of each compound in the two buffers, PB and BRB, were collected by exciting at a wavelength where the absorbances were equal in the two cases (300 nm for Δ^9-THCA and CBDA and 275 nm for Δ^9-THC and CBD), to allow direct comparison of the emission intensity in the two buffered solutions.

Δ^9-THCA and CBDA exhibit similar emission properties (Fig. 4A and

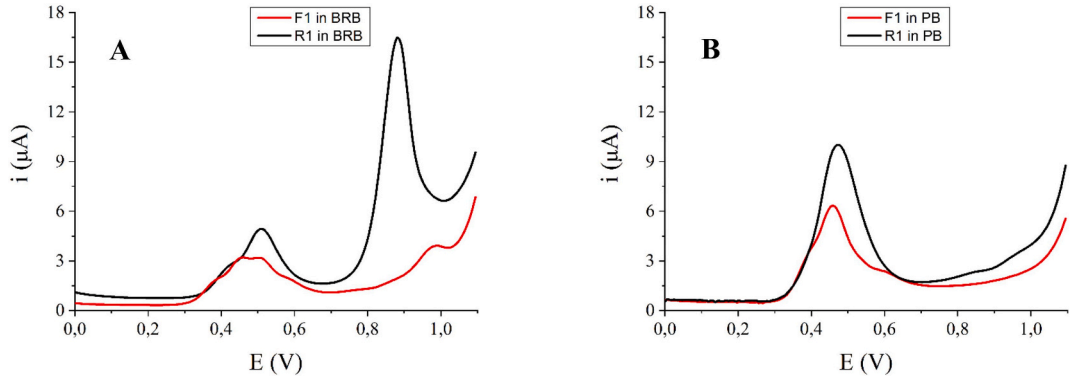

Fig. 3. DPV signals recorded using SPE-CB in R1 and F1 *C. sativa* extracts diluted in 7:3 *v*/v mixture of A) BRB (pH = 7.0) and EtOH, 0.1 M KCl; B) PB (pH = 7.0) and EtOH, 0.1 M KCl.

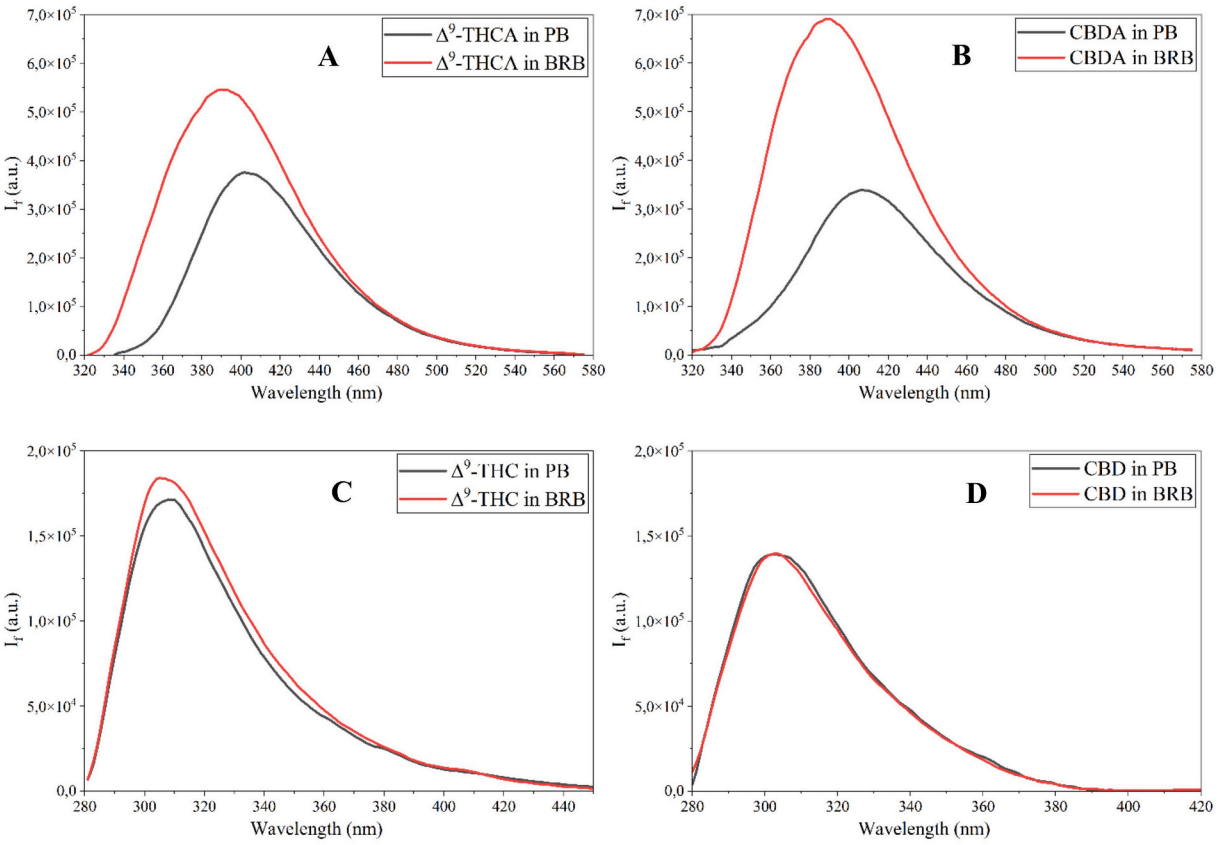

Fig. 4. Fluorescence spectra recorded on 7:3 v/v mixture of 0.024 M BRB or 0.01 M PB (both at pH = 7.0) and EtOH in the presence of A) 28 μM Δ^9-THCA, B) 28 μM CBDA, C) 95 μM Δ^9-THC and D) 28 μM CBD. λ_{exc} = 300 nm for Δ^9-THCA and CBDA spectra; λ_{exc} = 275 nm for Δ^9-THC and CBD spectra.

B). In PB both compounds exhibit the fluorescence maximum at ≈ 405 nm, whereas in BRB the maximum results blue-shifted to ≈ 395 nm. Furthermore, in BRB a broadening of the emission spectra and a marked increase in emission intensity compared to PB are observed. The value of the ratio between the integrated emission spectra in BRB and PB is 2.0 for CBDA, i.e., the fluorescence quantum yield of CBDA in BRB is twice that in PB. The corresponding ratio of Δ^9-THCA in BRB and PB is 1.6. The intensity, width and position of the fluorescence bands indicate that different species, characterized by distinct spectroscopic properties, are present in BRB compared to PB.

A few studies concerning the absorption and fluorescence spectra of cannabinoids are reported in the literature [32–34]. The spectra were collected in mixtures of organic solvents (acetonitrile or methanol) and aqueous buffers at nearly neutral or acidic pH. Since the fluorescence spectra of Δ^9-THCA and CBDA in PB, obtained in the present work, resemble those obtained in ethanol and acetonitrile/PB buffer at pH = 7.5 [32–34], showing a maximum at 405 nm, we can infer that no specific interactions take place between the compound and aqueous PB, and that the observed spectra can be attributed to the solvated species in a polar solvent. More specifically, although the presence of different conformers of cannabinoid compounds in solution cannot be excluded, the experimental observations, based on absorption and emission measurements, and in particular the independence of the fluorescence spectrum from the excitation wavelength (Figures SI 7), point to the presence of a dominant solvated species in PB, with a fluorescence maximum at about 405 nm, or to the presence of several conformers

with very similar spectroscopic properties.

The blue shift of the spectra and the enhancement of the fluorescence intensity of Δ^9-THCA and CBDA in BRB suggest that new species, characterized by different fluorescence properties, are formed in this buffer solution. This hypothesis is confirmed by the dependence of the fluorescence spectra on the excitation wavelength, observable only in BRB (Figures SI 8). This result indicates that at least two chemical species are present in this buffer: in addition to the species observed in PB possessing a fluorescence maximum at about 405 nm, attributable to the solvated species that do not specifically interact with the solvent, a second one, detectable in BRB solution, with a blue-shifted fluorescence maximum, is attributable to a species undergoing a specific interaction with boric acid.

In contrast to Δ^9-THCA and CBDA, Δ^9-THC (Fig. 4C) and CBD (Fig. 4D) do not show significant differences in terms of intensity and position of the emission peaks in the two buffers. Their fluorescence spectra are similar to each other and characterized by a maximum at about 300 nm, independent of the buffer and of the excitation wavelength in both buffers. This result points out that for these compounds only one fluorescent species is present in both buffer solutions and that no specific interaction takes place.

The hypothesis concerning the formation of a complex with boric acid was verified by the analysis of the absorption and fluorescence spectra of acidic cannabinoids in BRB at increasing boric acid concentration. UV–vis absorption and fluorescence spectra of a Δ^9-THCA solution were recorded, starting from diluted BRB (0.012 M and 0.004 M H_3BO_3) and progressively adding boric acid from a concentrated aqueous solution (Fig. SI9). A meaningful quantitative comparison of the fluorescence spectra, obtained by excitation at 300 nm, where the absorbance remained unchanged upon the addition of boric acid, was performed.

A slight red-shift of the absorption spectrum and the conservation of two isosbestic points at 263 and 288 nm can be observed up to a boric acid concentration of 0.020 M. The fluorescence spectrum is progressively blue-shifted, from 395 to 368 nm, and shows a marked increase in fluorescence intensity with increasing boric acid concentrations. On the basis of both absorption and emission spectral properties, we can infer that in BRB an equilibrium takes place between Δ^9-THCA and the Δ^9-THCA-boric acid complex, with a progressive shift of the equilibrium toward complex formation as the boric acid concentration increases.

The analysis of the absorption and emission spectra of CBDA, obtained in BRB upon addition of boric acid, leads to similar observations (Figures SI 10). Whereas the absorption spectrum of CBDA shows a slight red-shift, the fluorescence spectrum is blue-shifted from 395 to 380 nm, and the fluorescence intensity markedly increases. On the contrary, the absorption and fluorescence spectra of Δ^9-THC and CBD do not show any appreciable change in BRB upon the addition of boric acid. These results confirm the results of the electrochemical measurements, namely the occurrence of a specific interaction between H_3BO_3 and the acidic cannabinoids Δ^9-THCA and CBDA.

3.4. ^{11}B NMR study

The ^{11}B NMR measurements confirmed the formation of the boron complex with both Δ^9-THCA and 2,5-DHBA, as shown in Fig. 5. Indeed, similarly to salicylic acid [35], upon the addition of Δ^9-THCA to H_3BO_3 solution ($[H_3BO_3] = 15[\Delta^9\text{-THCA}]$) a new upfield shifted ^{11}B signal is observed at 2.9 ppm (Fig. 5B) with respect to the signal of free H_3BO_3 observed at 19.8 ppm (Fig. 5A). A similar behaviour is observed for 2,5-DHBA (Fig. 5C). It should be noted that the spectra in Fig. 5 were displayed using different vertical scales in order to highlight the diagnostic signal of the boron complex at 2.9 ppm, particularly in the case of Δ^9-THCA, whose concentration was 15-fold lower than that of 2,5-DHBA. Therefore, the apparent differences in the intensity of the residual free-boric-acid signal at 19.8 ppm among the spectra should not be considered quantitatively comparable. The higher intensity of the

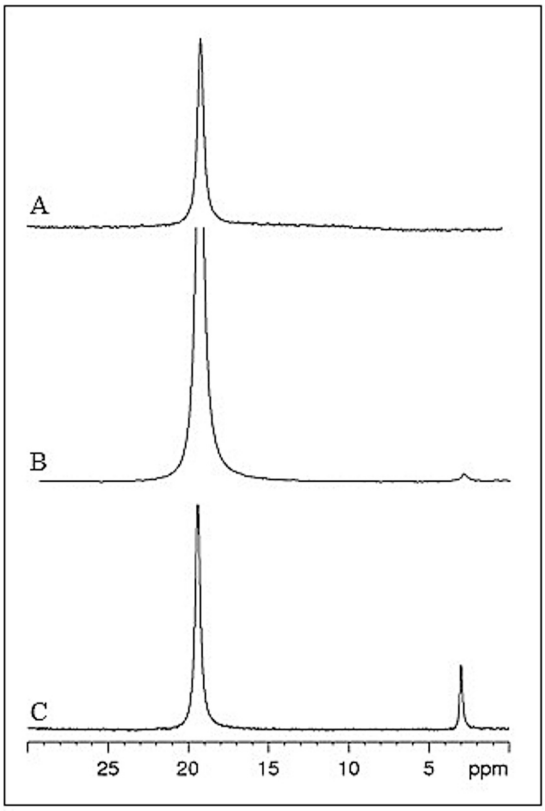

Fig. 5. ^{11}B NMR spectra of: A) H_3BO_3 (20 mM); B) H_3BO_3 (20 mM) in presence of Δ^9-THCA (1.3 mM); C) H_3BO_3 (10 mM) in presence of 2,5-DHBA (20 mM). Spectra were registered in PB (0.1M)/ACN (70:30 v/v) spiked with D_2O (50 μL) at 298 K (600 MHz).

boron-complex signal at 2.9 ppm observed for 2,5-DHBA is consistent with the different ligand-to-boron ratio used in this experiment, namely $2[H_3BO_3] = [2,5\text{-DHBA}]$, compared with $[H_3BO_3] = 15[\Delta^9\text{-THCA}]$ for Δ^9-THCA.

As previously stated [35], the ^{11}B NMR signal at 2.9 ppm corresponds to the 1-to-1 boron-to-ligand complex in which both carboxylate and phenolate oxygen atoms chelate boron. Even when the ligand concentration was twice that of boron, as in the case of 2,5-DHBA (Fig. 5C) only 14% of boron was bound to the ligand, forming the 1-to-1 complex. These data are consistent with low values of the formation constant ($\log K_{BL}$), as observed for salicylic acid ($\log K_{BL} = 1.05$). The formation of the 1-to-2 boron-to-ligand species characterized by a ^{11}B NMR signal at 3.3 ppm [35] was not been observed for either ligand.

4. Conclusions

This work demonstrates that boric acid plays a decisive role in modulating the electrochemical behaviour of acidic cannabinoids. Through a combined voltammetric, fluorometric, and ^{11}B NMR analysis, it has been demonstrated that Δ^9-THCA and CBDA selectively form stable tetrahedral borate complexes at neutral pH, whereas their neutral analogues, Δ^9-THC and CBD, do not exhibit comparable interactions. This differential boron complexation modulates both the redox and photophysical behaviours of the acidic cannabinoids, generating distinctive and analytically exploitable signal patterns.

The emergence of a high-potential anodic peak in borate-containing buffer, absent in phosphate medium and not observed for neutral cannabinoids, is directly attributable to borate coordination. UV–vis titrations allowed to calculate for the first time the proton dissociation constants of Δ^9-THCA and from the species distribution curves to

establish the predominance of the monoanionic form, i.e. the carboxylate one. Consistently, fluorescence measurements revealed blue-shifted, intensity-enhancement, and excitation-dependent emission profiles in borate buffer, indicative of multiple emissive species arising from complex formation. Direct spectroscopic evidence of boron complex formation is provided by ^{11}B NMR, which confirms the presence of a tetrahedral borate species coordinated by the acidic cannabinoids through both the carboxylate and phenate groups, through a two-step mechanism mediated by the anchoring group.

Collectively, these findings elucidate the molecular basis of borate-induced signal differentiation and rationalize the enhanced electrochemical discrimination of acidic cannabinoids in boric acid media. Beyond mechanistic insight, this work establishes a chemically grounded framework for the rational design of boron-assisted electroanalytical methods for the detection of cannabinoids, with direct implications for forensic analysis, regulatory control, and the development of rapid on-site screening methodologies for cannabis-derived products.

CRediT authorship contribution statement

Filippo Lugli: Writing – original draft, Investigation, Data curation. **Alessandro Monari:** Investigation, Data curation. **Monica Caselli:** Writing – review & editing, Writing – original draft, Methodology, Investigation, Funding acquisition. **Erika Ferrari:** Writing – review & editing, Writing – original draft, Methodology, Investigation. **Davide Vanossi:** Writing – review & editing, Funding acquisition. **Iuri Camilli:** Investigation. **Martina Campi:** Investigation. **Laura Pigani:** Writing – review & editing, Writing – original draft, Supervision, Methodology, Funding acquisition, Conceptualization.

Declaration of competing interest

The authors declare that they have no known competing financial interests or personal relationships that could have appeared to influence the work reported in this paper.

Acknowledgments

The Authors would like to thank the “Centro Interdipartimentale Grandi Strumenti - C.I.G.S.” of the University of Modena and Reggio Emilia (https://www.cigs.unimore.it) for NMR spectrometer and their precious technical support.

L.P., M.C., D.V. and F.L. thank the Department of Chemical and Geological Sciences for the financial support in the frame of “FAR Dipartimentale 2024”.

Appendix A. Supplementary data

Supplementary data to this article can be found online at https://doi.org/10.1016/j.microc.2026.119269.

Data availability

Data will be made available on request.

References

[1] X. Cetó, F. Maria Truta, A.M. Dragan, E. Rodríguez-Franch, M. Tertis, Á. Sánchez-Pereña, S. Comellas-Tena, C. Cristea, M. del Valle, Towards the development of a portable device based on modified-voltammetric sensors for the detection of illicit drugs and seized samples, Talanta 282 (2025) 127055, https://doi.org/10.1016/j.talanta.2024.127055.

[2] European Union Drugs Agency, European drug report 2024, in: European drug report (Online), LU: Publications Office, 2024. Accessed: Jan. 26, 2026. Available: https://data.europa.eu/doi/10.2810/91693.

[3] S.R. Wachtel, M.A. ElSohly, S.A. Ross, J. Ambre, H. de Wit, Comparison of the subjective effects of Δ^9-tetrahydrocannabinol and marijuana in humans, Psychopharmacology (Berl.) 161 (2002) 331, https://doi.org/10.1007/s00213-002-1033-2.

[4] S.C. Britch, S. Babalonis, S.L. Walsh, Cannabidiol: pharmacology and therapeutic targets, Psychopharmacology (Berl.) 238 (2021) 9, https://doi.org/10.1007/s00213-020-05712-8.

[5] M.M. Radwan, S. Chandra, S. Gul, M.A. ElSohly, Cannabinoids, phenolics, terpenes and alkaloids of cannabis, Molecules 26 (2021) 2774, https://doi.org/10.3390/molecules26092774.

[6] A. Singh, A. Bilichak, I. Kovalchuk, The genetics of Cannabis—genomic variations of key synthases and their effect on cannabinoid content, Genome 64 (2012) 490, https://doi.org/10.1139/gen-2020-0087.

[7] D.J. Potter, P. Clark, M.B. Brown, Potency of Δ^9-THC and other cannabinoids in cannabis in England in 2005: implications for psychoactivity and pharmacology*, J. Forensic Sci. 53 (2008) 90, https://doi.org/10.1111/j.1556-4029.2007.00603.x.

[8] D.J. Potter, K. Hammond, S. Tuffnell, C. Walker, M. Di Forti, Potency of Δ9-tetrahydrocannabinol and other cannabinoids in cannabis in England in 2016: implications for public health and pharmacology, Drug Test. Anal. 10 (2018) 628, https://doi.org/10.1002/dta.2368.

[9] G. Appendino, G. Chianese, O. Taglialatela-Scafati, Cannabinoids: occurrence and medicinal chemistry, Curr. Med. Chem. 18 (2011) 1085, https://doi.org/10.2174/092986711794940888.

[10] B.F. Thomas, M.A. ElSohly, The Analytical Chemistry of Cannabis: Quality Assessment, Assurance, and Regulation of Medicinal Marijuana and Cannabinoid Preparations, 1st ed, Elsevier, 2015, https://doi.org/10.1016/C2014-0-03861-0. ISBN: 978-0-12-804646-3.

[11] J.A. Hartsel, J. Eades, B. Hickory, A. Makriyannis, Chapter 53 - *Cannabis sativa* and Hemp, Editor(s): Ramesh C. Gupta, Nutraceuticals, Academic Press, 2016, Pages 735–754, ISBN 9780128021477, doi:https://doi.org/10.1016/B978-0-12-802147-7.00053-X.

[12] C.M. Andre, J.-F. Hausman, G. Guerriero, *Cannabis sativa: the plant of the thousand and one molecules*, Front. Plant Sci. 7 (1) (2016), https://doi.org/10.3389/fpls.2016.00019.

[13] R. Mechoulam, L.O. Hanuš, R. Pertwee, A.C. Howlett, Early phytocannabinoid chemistry to endocannabinoids and beyond, Nat. Rev. Neurosci. 15 (2014) 757, https://doi.org/10.1038/nrn3811.

[14] B. De Backer, B. Debrus, P. Lebrun, L. Theunis, N. Dubois, L. Decock, A. Verstraete, P. Hubert, C. Charlier, Innovative development and validation of an HPLC/DAD method for the qualitative and quantitative determination of major cannabinoids in cannabis plant material, J. Chromatogr. B 877 (2009) 4115, https://doi.org/10.1016/j.jchromb.2009.11.004.

[15] B. Zanfrognini, L. Pigani, C. Zanardi, Recent advances in the direct electrochemical detection of drugs of abuse, J. Solid State Electrochem. 24 (2020) 2603, https://doi.org/10.1007/s10008-020-04686-z.

[16] M. Renaud-Young, R.M. Mayall, V. Salehi, M. Goledzinowski, F.J.E. Comeau, J. L. MacCallum, V.I. Birss, Development of an ultra-sensitive electrochemical sensor for Δ^9-tetrahydrocannabinol (THC) and its metabolites using carbon paper electrodes, Electrochim. Acta 307 (2019) 351, https://doi.org/10.1016/j.electacta.2019.02.117.

[17] R. Nissim, R.G. Compton, Absorptive stripping voltammetry for cannabis detection, Chem. Cent. J. 9 (2015) 41, https://doi.org/10.1186/s13065-015-0117-0.

[18] E.R. Darzi, N.K. Garg, Electrochemical oxidation of Δ9-tetrahydrocannabinol: a simple strategy for marijuana detection, Org. Lett. 22 (2020) 3951, https://doi.org/10.1021/acs.orglett.0c01241.

[19] M.O. Brandão, L.C. Arantes, C.D. Lima, B.G. Lucca, N.C. Moraes, E.R. Pedão, F.M. R. Guerbas, S.S. Gebara, W.T.P. Dos Santos, Portable voltammetric method for the simultaneous determination of Δ^9-tetrahydrocannabinol and cannabidiol in alkaline medium using unmodified screen-printed carbon electrodes, Talanta 304 (2026) 129562, https://doi.org/10.1016/j.talanta.2026.129562.

[20] A. Monari, S. Cantalù, B. Zanfrognini, V. Brighenti, P. Verri, C. Zanardi, F. Pellati, L. Pigani, An electrochemical approach for the prediction of Δ9-tetrahydrocannabinolic acid and total cannabinoid content in *Cannabis sativa* L. Analyst 148 (2023) 4688, https://doi.org/10.1039/D3AN01090B.

[21] A. Monari, G. Foca, A. Ulrici, B. Zanfrognini, V. Brighenti, P. Verri, F. Pellati, C. Zanardi, L. Pigani, Electrochemical sensors for fast classification of different *Cannabis sativa* L. samples according to total Δ^9-tetrahydrocannabinol content, Talanta 282 (2025) 126958, https://doi.org/10.1016/j.talanta.2024.126958.

[22] Richard. Pizer, Lucia. Babcock, Mechanism of the complexation of boron acids with catechol and substituted catechols, Inorg. Chem. 16 (1997) 1677, https://doi.org/10.1021/ic50173a021.

[23] D. Köse, B. Zümreoglu-Karan, Mixed-ligand complexes of boric acid with organic biomolecules, Chem. Pap. 66 (2012) 54, https://doi.org/10.2478/s11696-011-0108-0.

[24] D.A. Köse, B. Zümreoglu-Karan, Complexation of boric acid with vitamin C, New J. Chem. 33 (2009) 1874, https://doi.org/10.1039/b902812a.

[25] D.A. Köse, B. Zümreoglu-Karan, T. Hökelek, E. Şahin, Boric acid complexes with organic biomolecules: mono-chelate complexes with salicylic and glucuronic acids, Inorg. Chim. Acta 363 (2010) 4031, https://doi.org/10.1016/j.ica.2010.08.001.

[26] D.A. Köse, B. Zümreoglu-Karan, T. Hökelek, A comparative examination of mono- and bis-chelate salicylatoborate complexes and the crystal structure of layered magnesium bis-salicylatoborate, Inorg. Chim. Acta 375 (2011) 236, https://doi.org/10.1016/j.ica.2011.05.012.

[27] C. Shao, S. Matsuoka, Y. Miyazaki, K. Yoshimura, T.M. Suzuki, D.A.P. Tanaka, Equilibrium and kinetic studies on the complexation of boric acid with chromotropic acid, J. Chem. Soc. Dalton Trans. 18 (2000) 3136, https://doi.org/10.1039/b004399k.

[28] A. Queen, The kinetics of the reaction of boric acid with salicylic acid, Can. J. Chem. 55 (1977) 3035, https://doi.org/10.1139/v77-421.
[29] M. Rafiee, D. Nematollahi, Electrochemical study of catechol-boric acid complexes, Electrochim. Acta 53 (2008) 2751, https://doi.org/10.1016/j.electacta.2007.10.055.
[30] H. Beiginejad, Z. Rafiee, M. Moradi, Electrochemical oxidation of caffeic acid in the presence of 1,4-benzenediboronic acid: CEC mechanism and glucose effect on the complex formation, J. Iran. Chem. Soc. 17 (2020) 935, https://doi.org/10.1007/s13738-019-01827-8.
[31] M. Rafiee, D. Nematollahi, H. Salehzadeh, CEC mechanism in electrochemical oxidation of nitrocatechol-boric acid complexes, Electrochim. Acta 56 (2011) 994652, https://doi.org/10.1016/j.electacta.2011.08.083.
[32] A. Hazekamp, A. Peltenburg, R. Verpoorte, C. Giroud, Chromatographic and spectroscopic data of cannabinoids from *Cannabis sativa* L. J. Liq. Chromatogr. Relat. Technol. 28 (2005) 2361, https://doi.org/10.1080/10826070500187558.
[33] M. Birenboim, Å. Rinnan, D. Kengisbuch, J.A. Shimshoni, Novel fluorescence spectroscopy coupled with PARAFAC modeling for major cannabinoids quantification and identification in cannabis extracts, Chemom. Intell. Lab. Syst. 232 (2023) 104717, https://doi.org/10.1016/j.chemolab.2022.104717.
[34] M. Birenboim, E. Fallik, D. Kengisbuch, J.A. Shimshoni, Quantitative and qualitative spectroscopic parameters determination of major cannabinoids, J. Lumin. 252 (2022) 119387, https://doi.org/10.1016/j.jlumin.2022.119387.
[35] Y. Miyazaki, H. Matsuo, T. Fujimori, H. Takemura, S. Matsuoka, T. Okobira, K. Uezu, K. Yoshimura, Interaction of boric acid with salicyl derivatives as an anchor group of boron-selective adsorbents, Polyhedron 27 (2008) 2785, https://doi.org/10.1016/j.poly.2008.06.007.
[36] D. López-Iglesias, J.J. García-Guzmán, C. Zanardi, J.M. Palacios-Santander, L. Cubillana-Aguilera, L. Pigani, Fast electroanalytical determination of cannabidiol and cannabinol in aqueous solution using Sonogel-Carbon-PEDOT devices, J. Electroanal. Chem. 878 (2020) 114591, https://doi.org/10.1016/j.jelechem.2020.114591.
[37] M. Cirrincione, B. Zanfrognini, L. Pigani, M. Protti, L. Mercolini, C. Zanardi, Development of an electrochemical sensor based on carbon black for the detection of cannabidiol in vegetable extracts, Analyst 146 (2021) 612–619, https://doi.org/10.1039/D0AN01932A.
[38] P. Gans, A. Sabatini, A. Vacca, Investigation of equilibria in solution. Determination of equilibrium constants with the HYPERQUAD suite of programs, Talanta 43 (1996) 1739–1753, https://doi.org/10.1016/0039-9140(96)01958-3.
[39] L. Alderighi, P. Gans, A. Ienco, D. Peters, A. Sabatini, A. Vacca, Hyperquad simulation and speciation (HySS): a utility program for the investigation of equilibria involving soluble and partially soluble species, Coord. Chem. Rev. 184 (1999) 311, https://doi.org/10.1016/S0010-8545(98)00260-4.
[40] L. Castellino, E. Alladio, S. Bertinetti, G. Lando, C. De Stefano, S. Blasco, E. García-España, S. Gama, S. Berto, D. Mileaet, PyES - an open-source software for the computation of solution and precipitation equilibria, Chemom. Intell. Lab. Syst. 239 (2023) 104860, https://doi.org/10.1016/j.chemolab.2023.104860.
[41] R. Stewart, M.R. Granger, The basicities of ortho-substituted benzoic acids, Can. J. Chem. 39 (1961) 2508–2515, https://doi.org/10.1139/v61-33.
[42] Z.M. Robole, K.L. Rahn, B.J. Lampkin, R.K. Anand, B. VanVeller, Tuning the electrochemical redox potentials of catechol with boronic acid derivatives, J. Org. Chem. 84 (2019) 2346, https://doi.org/10.1021/acs.joc.8b03087.